Desalination and Water Treatment
www.deswater.com

doi: 10.5004/dwt.2019.23535

144 (2019) 156–165
March

Synthesis of zeolite LTA using an agro-industrial residue as the SiO_2 precursor and evaluating its effectiveness in the removal of copper ions from water

Luis Mario González-Rodríguez[a], Nicolás Alán Pérez-Durán[a], Margarita Loredo-Cancino[b], Gerardo Antonio Flores-Escamilla[b], David Alejandro De Haro-Del Río[b,*]

[a]*Instituto Politécnico Nacional, Unidad Profesional Interdisciplinaria de Ingeniería Campus Zacatecas, Zacatecas, C.P. 98160, México, emails: lmgonzalezr@ipn.mx (L.M. González-Rodríguez), alanpduran@gmail.com (N.A. Pérez-Durán)*
[b]*Universidad Autónoma de Nuevo León, UANL, Facultad de Ciencias Químicas, Av Universidad S/N, Cd. Universitaria, San Nicolás de los Garza, N. L. C.P. 64451, México, emails: dharodlr@uanl.edu.mx (D.A. De Haro-Del Rio), margarita.loredocn@uanl.edu.mx (M. Loredo-Cancino), gerardo.florescm@uanl.edu.mx (G.A. Flores-Escamilla)*

Received 31 August 2018; Accepted 26 November 2018

ABSTRACT

This paper deals with the synthesis and characterization of zeolite type A (ZA) using an agro-industrial residue such as barley husk as ecological and nonexpensive silica (SiO_2) precursor. The amorphous silica phase was achieved by pyrolysis and then was used to form a synthetic gel in a typical hydrothermal procedure where the carbonaceous phase was removed by calcination afterwards. The characterization of prepared materials by X-ray diffraction, scanning electron microscopy, and energy-dispersive X-ray spectroscopy techniques was carried out. ZA was evaluated in the removal of copper ions from water by atomic absorption spectrophotometry. Also, kinetic studies by using pseudo-first-order (PFO) and pseudo-second-order models were carried out to evaluate the performance of ZA. The PFO model showed a better approximation for ZA data. Finally, thermodynamic equilibrium was well represented by Langmuir and Freundlich models achieving a maximum adsorption capacity of 143.9 mg g^{-1}.

Keywords: Zeolite LTA; Barley husk ash; Revalorization; Copper adsorption; Kinetic models

1. Introduction

Industrial activities are mainly responsible for the release of heavy metals to the environment. Heavy metals are defined as chemical elements that exceed 5 g cm^{-3} in density and have atomic weights in the range of 63.5–200.6 [1,2]. Unlike organic pollutants, heavy metals are nonbiodegradable and tend to accumulate in organisms as elements in the food chain. Many metals can be classified as heavy metals; however, those that represent a major threat to humans and other living organisms due to their toxicity are arsenic, cobalt, cadmium, chromium, copper, nickel, lead, mercury, and zinc [3,4]. Although copper is an essential element for the human metabolism playing a key role in the reproductive system, its exposure and ingestion in acute doses can cause poisoning as gastric and intestinal stresses, hemolytic anemia, neurological abnormalities, and corneal opacity [5–7]. Sources of copper in wastewater bodies have their origin in several sources such as mining and smelting activities, pigment industry, and electroplating [8].

Different methods such as precipitation, coagulation/flocculation, osmosis, and electrolysis have been applied to prevent and solve problems related to heavy metal disposal in water bodies with certain success level. However, the main drawbacks using these technologies include the generation of large volume of toxic sludge, high energy consumption, operational costs, and lack of selectivity. Adsorption is currently the most promising technology in the removal of toxic metals from water because of its easiness in implementation and high efficiency. However, it still has some drawbacks like materials' cost and regeneration [9].

* Corresponding author.

Zeolites are crystalline aluminosilicates possessing micropores composed of TO_4 tetrahedra (T = Si or Al) and ion-exchange capabilities. Ion exchange in zeolites occurs because of the presence of the AlO_4^- tetrahedra in the framework, which are neutralized by ions or protons that are easily exchangeable [10]. These characteristics have allowed zeolites to be used as adsorbents and catalysts. One of the most used zeolites in industry as cation adsorbent is the well-known zeolite type A (ZA) (Linde type A, LTA). This structured material has a relative low-density framework (12.9 T-atoms/1,000 Å^3) which provides larger volume to adsorb species within their porous network. Also, LTA has a low Si/Al ratio (~1) having an increased aluminum content which represents a higher number of exchangeable cations [11]. Few studies of Cu adsorption on LTA zeolite are reported. Elsayed-Ali et al. [12] investigated the adsorption of copper (II) in water with a synthetic LTA zeolite and an electrokinetic cell using carbon electrodes. However, despite the effective removal of the contaminant (~84%), they found that chemical interactions lead to the precipitation of copper oxide on the zeolite surface. Also, the use of an electric field would increase the cost of the process. Synthetic zeolites are commonly prepared following the hydrothermal route, i.e., a series of heterogeneous reactions that usually are carried out using a solvent in a range of pressure and temperature levels depending upon the type of material to be produced [13]. The required species for the formation of zeolites are typically a source of silica (SiO_2), a source of alumina (Al_2O_3), an alkaline media, and water as solvent [13]. Despite silicon is the most abundant element on earth surface, most of the silica used as precursor in the synthesis of many industrial applications is produced by synthetic means. The natural chemical composition of certain kind of agro-industrial by-products, specifically the amount of SiO_2, plays a crucial role to be used as replacement of the traditional sources providing an alternative to replace commercial silica precursors facilitating to revalorize a residue [14].

Currently, a large volume of solid wastes is generated by agro-industrial activities around the world. According to recent figures from Food and Agricultural Organization, the production of food wastes ascends to 1.3 billion t year^{-1} [15]. These residues have been used as animal fodder or they are disposed in the landfill or simply burnt. However, it has been reported that some residues having high concentration of SiO_2 could be difficult to digest by animals and have low nutritional value [16]. Recently, the residues have been used to produce biofuels by fermentation-distillation routes. [16]. Also, higher SiO_2 content in lignocellulosic materials represents a drawback in the biofuel production due to the generation of a secondary source of pollution, and its removal can be costly or harsh for the environment [17].

Rice husk ash possesses superior levels of amorphous silica (up to 98%), and it has been the most widely used residue for the production of synthetic zeolite structures such as LTA [18], mordenite [19], faujasite (FAU) [16], hexagonal faujasite [14], BEA [20], edigontite [21], and zeolite socony mobil-5 [22]. These materials have been prepared by modifying synthetic parameters such as temperature, crystallization time, and SiO_2/Al_2O_3 ratio among others leading to different morphologies and particle sizes, including nanosized materials. The prepared zeolites have found diverse applications such as hydrocarbon adsorption and environmental technologies. Further, zeolite analcime, which can be found in nature, has also been prepared using rice husk for catalytic applications [23].

In the same sense towards the revalorization of residual materials, recently, other different agro-residues have raised attention as sugar cane bagasse [24], corn cob [25], wheat [26], and bamboo [27]. The pyrolysis-obtained char has been used as silica source to synthesize zeolite types LTA, pressure (*P*), and FAU by the hydrothermal method. Also, it has been described that char is a more favorable precursor for certain applications such hydrothermal routes, as additional natural compounds do not intervene in the crystallization stage [16]. Barley is the fourth most abundant cereal in the world with a production of about 150 million t. The most important uses of barley include malting, brewing, and cattle feed [28]. Barley husk is a residue obtained during the cleaning stages in the barley malting. It has been reported that silica content in barley husk ranges from 50%–80% [29].

The aim of this study was to produce a zeolitic material by the revalorization of an agro-industrial residue with the capability to remove copper ions (Cu^{2+}) from aqueous media. Specifically, barley husk was used as silica precursor of LTA zeolite type. The residue was pyrolyzed in order to obtain an amorphous silica phase and consequently being used directly in a hydrothermal procedure. In summary, in this study, an alternative to contribute in the minimization of solid residues is proposed, turning them into a functional material able to be applied in environmental technologies.

2. Methodology

2.1. Synthesis of zeolitic materials

A traditional synthetic zeolite LTA (TZA) was synthesized from commercial Na_2SiO_3; meanwhile, other zeolite was prepared using a lignocellulosic residue as SiO_2 precursor (BHZA). TZA material was synthesized by the hydrothermal method following the gel composition $3Na_2O{:}0.85SiO_2{:}Al_2O_3{:}180H_2O$ [30]. In a typical run, a solution with 4.00 g of NaOH (≥98%, Sigma-Aldrich, USA) in 50 mL of distilled water was prepared; it was stirred until homogenized and divided into two equal parts. Then, 2.6023 g of $Al(OH)_3$ (Sigma-Aldrich, USA) was added to 25 mL of the prepared NaOH solution and stirred for 1 h. Further, SiO_2 precursor, 3.9639 g of Na_2SiO_3 (Aldrich), was added to the remaining 25 mL of NaOH solution and mixed until homogenization. Both prepared solutions were mixed and stirred for 24 h at room temperature in a closed container to obtain a gel, which is highly alkaline up to pH 14. Then, the gel was transferred to a Teflon-lined stainless steel autoclave to carry out the crystallization process in an oven at 100°C for 4 h. After cooling for an hour, the product was recovered by vacuum filtration and washed with deionized water until pH 8 was reached.

In the case of BHZA, first carbonization of barley husk (BHC) was carried out in a tubular furnace under 0.1 L min^{-1} nitrogen atmosphere, heating from room temperature to 200°C at a rate of 5°C min^{-1}, held for 2 h followed by ramping at 5°C min^{-1} to 600°C and held for 2 h. After this, the furnace was allowed to cool to room temperature. Then, similar hydrothermal procedure was carried out by substituting the Na_2SiO_3 by

1.59 g of BHC. The BHC amount contained the equivalent SiO_2 according to its compositional analysis, 50.3 wt.%, to complete the gel composition (see characterization section). Both final solids were dried at 80°C. In order to remove carbonaceous materials that were not *zeolitized*, it was calcinated up to 500°C for 6 h in a muffle furnace and it was labeled as ZA.

2.2. Characterization of zeolitic materials

A physicochemical characterization of materials was carried out. X-ray diffraction (XRD) was used to identify the crystalline phases of tested materials. This analysis was carried out with a Siemens D5000 X-ray diffractometer; samples were scanned within the 2θ angular range of 5°–50° with a step size of 0.020° and a time of 10 s at 25°C. Thermal degradation experiments in a simultaneous DSC-TGA analyzer (TA instruments SDT 2960, USA) were carried out. The sample was heated under nitrogen atmosphere from room temperature to 800°C at a heating rate of 10°C min^{-1}. Morphological analysis and elemental analysis were performed by scanning electron microscopy (SEM) with field emission and energy-dispersive X-ray spectroscopy (EDX), respectively, at 20 kV (JSM-7800F, JEOL, Japan). For SEM analysis, the samples were coated with a thin layer of gold using sputtering technique. Textural properties were determined using N_2 adsorption-desorption isotherms at 77 K, obtained with a TriStar II equipment (Micrometry, USA) device. Specific surface area was estimated with the Brunauer, Emmet, and Teller method (BET) in a range of partial (P/P_0) of 0–0.3 and average pore size by using the Barrett, Joyner, and Halenda method.

2.3. Adsorption tests – kinetics

Copper adsorption experiments with the three prepared materials TZA, BHZA, and ZA were carried out. A 0.5 g of each material was added into 40 mL of $Cu(NO_3)_2$ solution with initial concentration of 400 ppm and continuous stirring during a period of 5, 10, 20, 30, and 60 min. Prepared solutions of 0.1M NaOH and 0.1 M HCl were employed to adjust and maintain a constant pH of 4. Copper adsorption capacities (q, mg g^{-1}) of prepared materials were calculated with the mass balance equation: $q = (C_0\text{-}C) \times (V/m)$, where C_0 (mg L^{-1}) is the initial copper concentration, C (mg L^{-1}) is the copper concentration after adsorption at time t (h), V (L) is the solution volume, and m (g) is the adsorbent mass. After the copper adsorption process, the zeolites were separated by centrifugation and the copper concentration was quantified in the supernatant solution by atomic absorption spectrophotometry (Cintra GBC 942 AA, Australia) by direct aspiration into an air-acetylene flame at a flow rate of 0.4 mL min^{-1} using a wavelength of 327.5 nm.

Copper adsorption over prepared materials was characterized with common kinetic and isotherm adsorption equations widely used for zeolites. Pseudo-first-order (PFO) [31] and pseudo-second-order (PSO) [32] equations were utilized for data fitting of copper adsorption kinetics. These two models assume a reaction-controlled process and are defined as $dq_{PFO}/dt = k_1(q_{e,PFO} - q_{PFO})$ and $dq_{PSO}/dt = k_2(q_{e,PSO} - q_{PSO})^2$, where q_{PFO} and q_{PSO} are the copper adsorption capacities estimated by the kinetic models in mg g^{-1}, k_1 is the PFO rate constant in min^{-1}, and k_2 is the PSO rate constant in g mg^{-1} min.

2.4. Adsorption tests – equilibrium

To correlate the copper adsorption isotherms over the prepared materials, Langmuir [33] and Freundlich [34] equations were employed: $q_{e,L} = q_{m,L}K_LC_e/(1 + K_LC_e)$ and $q_{e,F} = k_nC_e^{\frac{1}{n_F}}$, where q_e is the equilibrium adsorption capacity (mg g^{-1}), C_e is the copper equilibrium concentration (mg L^{-1}), $q_{m,L}$ is the monolayer adsorption capacity in mg g^{-1}, K_L is the Langmuir constant in L mg^{-1}, and k_n (mg$^{1-1/n}$ L$^{1/n}$ g^{-1}) and n_F are the respective parameters of Freundlich isotherm. Parameters were estimated from experimental data by using the nonlinear model forms, and the used objective function was the minimization of the sum of squares of error applying the Generalized Reduced Gradient (GRG2) Algorithm. The coefficient of determination R^2 was used to test the model fitting.

3. Results and discussion

3.1. Characterization results

Thermogravimetric analysis of the raw barley husk in Fig. 1 shows that the major thermal decomposition occurred in the range of 300°C–700°C. This weight loss is due to the release of light volatile compounds from the degradation of cellulose, hemicellulose, and lignin. The final product, thermally stable at temperatures above 700°C, was considered as ash. It has been previously reported that SiO_2 represents between 50 and 85 wt.% of the barley husk ash [29,35].

The carbonization processes of the raw barley husk produced the material named BHC. In Fig. 2, the corresponding SEM images for this material can be seen which revealed that BHC surface has a heterogeneous and fibrous surface and a morphology that resembles broken tubes. This type of morphology has been previously obtained using similar materials exposed to similar thermal treatments [36]. In the outer surface of these fibers, Fig. 2(a), it can be appreciated with a kind of coating with round structures, which are mainly composed of Si as EDX analysis revealed in Fig. 2(b). The averaged chemical composition for Si in this section of the materials is 50.3 wt.% (normalized). This silicon content

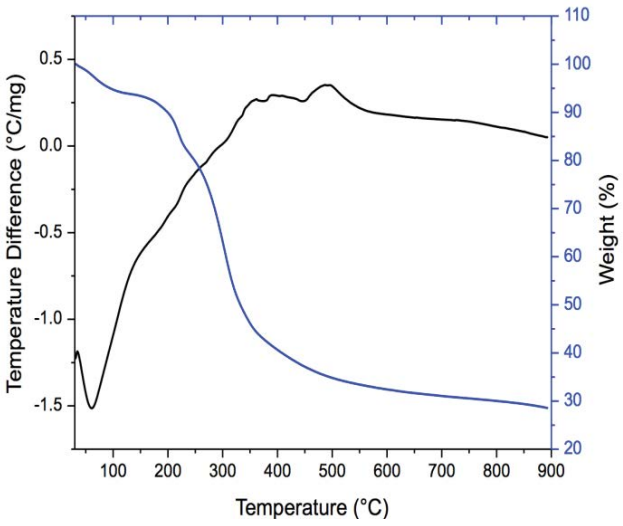

Fig. 1. TGA and DTA curves for raw barley husk.

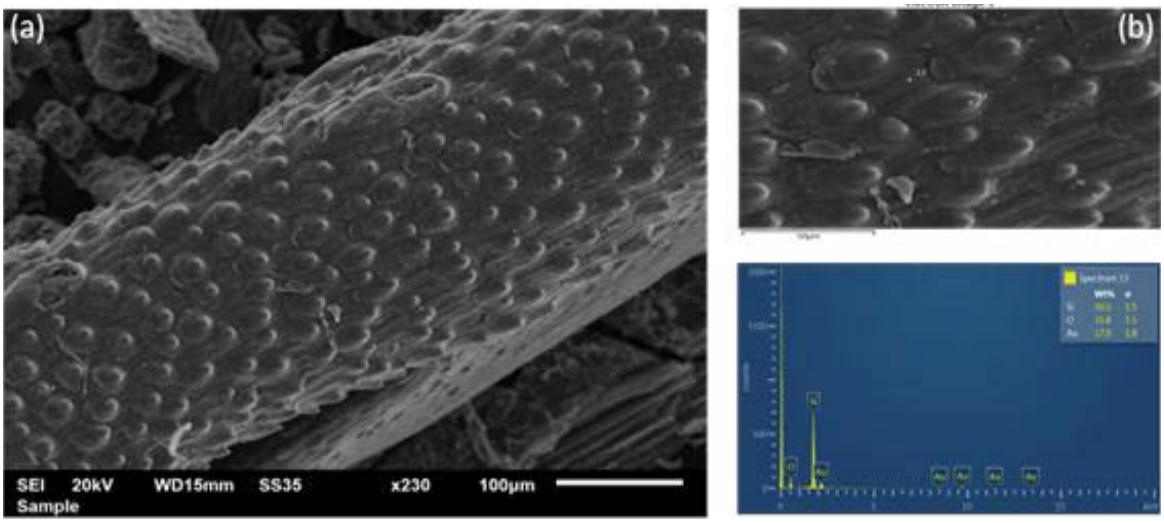

Fig. 2. SEM micrographs of carbonized barley husks. (a) Exterior parts of materials where reactive silica is observed (circular shapes) and (b) EDX analysis of identified points.

determined the initial zeolite gel composition to form the LTA structure. It should be noted that the presence of Au in the EDX spectrum is due to the sample preparation for the analysis. A summary with the elemental composition of all materials can be seen in Table 1.

On the other hand, part of the inner surface of fibers shows a rougher aspect as can be seen in Fig. 3(a). For this case, the elemental analysis revealed that it is composed mainly of carbon, up to 66.6 wt.% as EDX analysis revealed in Fig. 3(b).

Fig. 4 presents the nitrogen adsorption/desorption isotherm for the carbonized sample BHC. According to the International Union of Pure and Applied Chemistry classification, this isotherm exhibits a type I behavior, which is characteristic for microporous materials, i.e., pore diameter in the range of 2 nm and below. The generation of these types of pores can be attributed to the removal of volatile compounds after the thermal treatment. This type of isotherm is often seen in activated carbons. However, the surface area values are relative low, 40.7 $m^2 g^{-1}$, compared to those carbons that have been subject to an activation process.

Fig. 5 shows the SEM images of the materials after the hydrothermal treatment using the BHC as silicon source; this

Table 1
EDX-SEM elemental quantification for BHC (in and out sections), ZA, BHZA, and TZA (normalized)

Element	BHC (in)	BHC (out)	ZA	BZA	TZA
	Wt.%				
Si	2.2	50.3	21.9	5.1	14.5
Al	–	–	15.4	6.5	8.0
C	31.3	17.9	–	37.0	–
O	66.6	31.8	52.9	44.9	60.4
Na	–	–	9.7	6.4	17.2

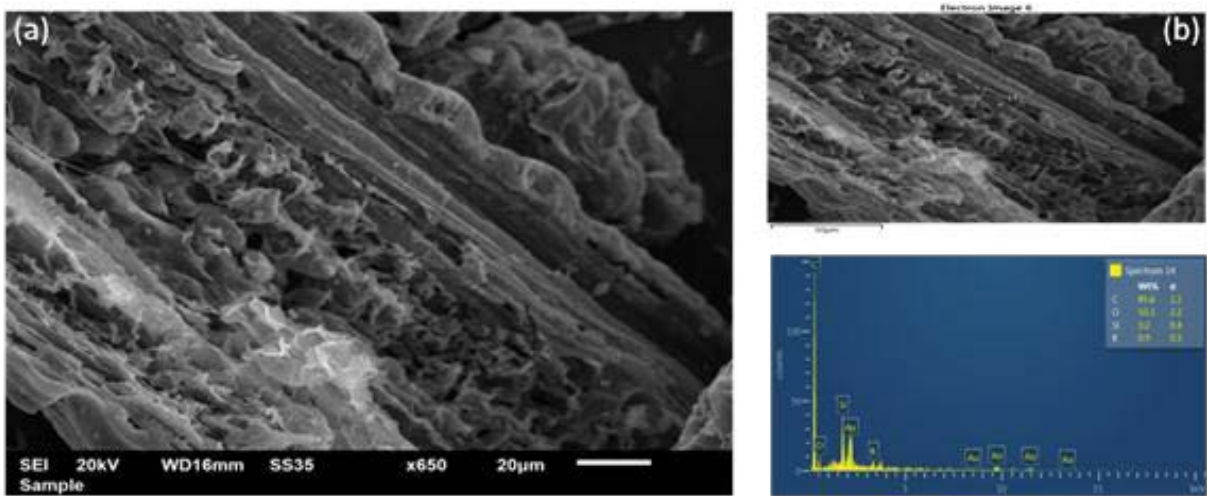

Fig. 3. (a) SEM micrographs of carbonized barley husk and (b) EDX analysis of identified points.

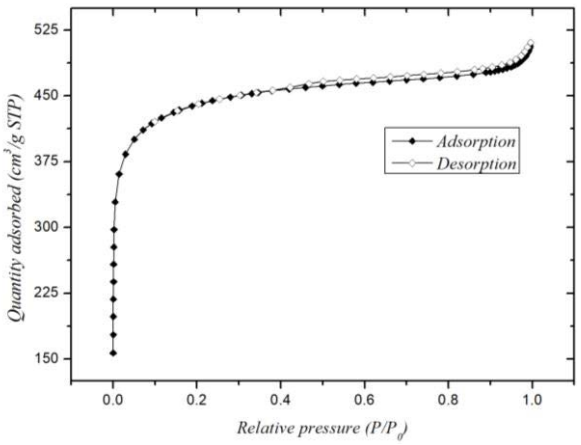

Fig. 4. Nitrogen physisorption of BHC.

material was labeled as BHZA. The hydrothermal process was successful in developing the characteristic cubic crystalline structure particles corresponding to LTA zeolite framework on the outer section of carbonized precursors. Formed crystals range from 1 to 2mm, which agrees with typical zeolite LTA preparations.

The formation of LTA framework is confirmed by the XRD pattern presented in Fig. 6(a) where the characteristic peaks for LTA can be observed at 7.1°, 10.1°, and 12.4° [11] along with a broad peak around 24°, commonly found in carbonaceous materials. In Fig. 7, the XRD pattern for TZA is shown; a high purity material exhibiting the totality of the peaks for the LTA framework can be clearly seen. The elemental analysis by EDX of BHZA in relative wt.% was C = 37.0%, O = 44.9%, Si = 6.5%, Na = 6.4%, and Al = 5.1%. The Si/Al ratio is 1.3, which is also an indicative of the formation of LTA zeolite type. However, the large carbon content on the composite seems to be related to the material lying under the zeolite as the precursor was mainly carbon, and it did not react in the hydrothermal procedure. It is clear that for BHZA, the presence of carbon lying under the zeolite layer plays a role in its structure. Additionally, it has been reported that the presence of carbonaceous material can affect the adsorption capacity for the removal of cations from water [37]. This is the main reason why carbon was removed after the carbonization procedure.

In Fig. 5(b), the nitrogen adsorption/desorption isotherm of BHZA is shown. Type IV isotherm can be observed, which is characterized by the hysteresis loop related to the formation of mesopores (2–50 nm pore diameter) in the material. This can be explained by the modification of carbonaceous materials which probably suffered an expansion of its porosity after the hydrothermal synthesis whilst zeolites contribute with the microporous features. A summary of textural properties can be seen in Table 1.

A yield of 9.57% was reached, i.e., from the original 58.19 g contained in the preparation gel, 5.56 g was obtained as BHZA. Then, after the carbon removal, 1.83 g of ZA was obtained as final product. In Fig. 8(a), the XRD pattern for the ZA material is shown; the peaks in the positions are also in agreement with the formation of LTA framework. In this case, the valley (15°–30°) in BHZA diffraction pattern is no longer present in the material, being this an indicative that the carbonaceous material was successfully removed from the composite, letting mainly only ZA in the material. This is also confirmed by EDX analysis where carbon was not detected as can be seen in Fig. 8(b). However, in Fig. 8(d), an SEM image of ZA shows that the particles' size and their morphologies are not uniform. This can be due to the thermal procedure used to remove the carbonaceous phase or associated with the presence of other mineral compounds that did not intervene in the zeolite formation such as calcium, magnesium, or potassium, as EDX analysis revealed in Fig. 8(b). This could lead to the formation of other crystallographic species, although their concentration

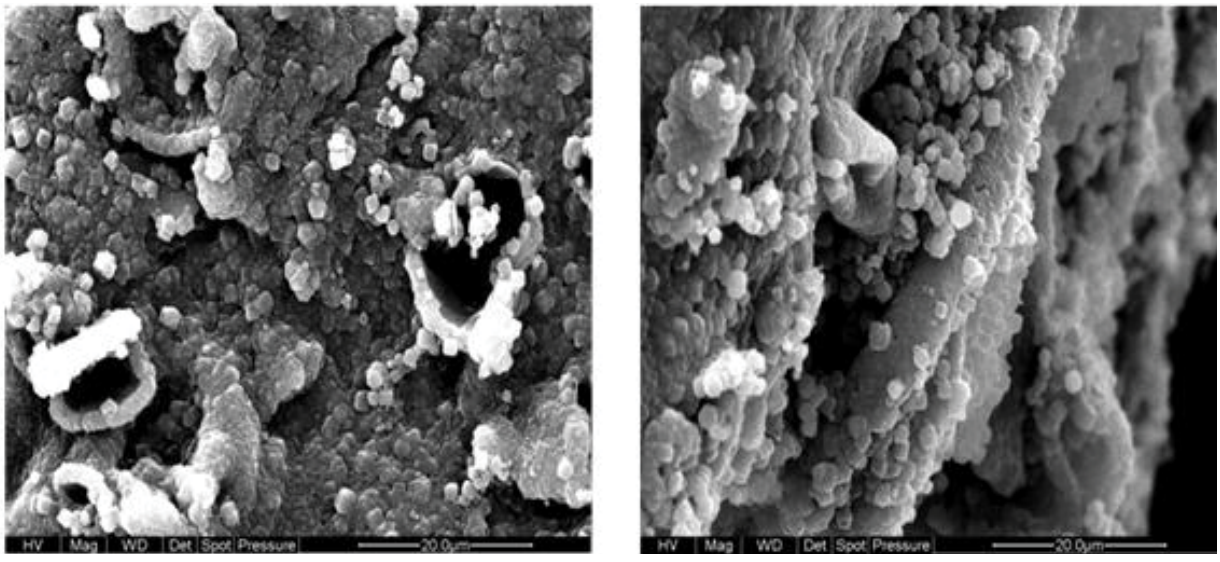

Fig. 5. SEM micrographs of zeolitic composite BHZA formed after the hydrothermal process using barley husk carbon as SiO_2 source.

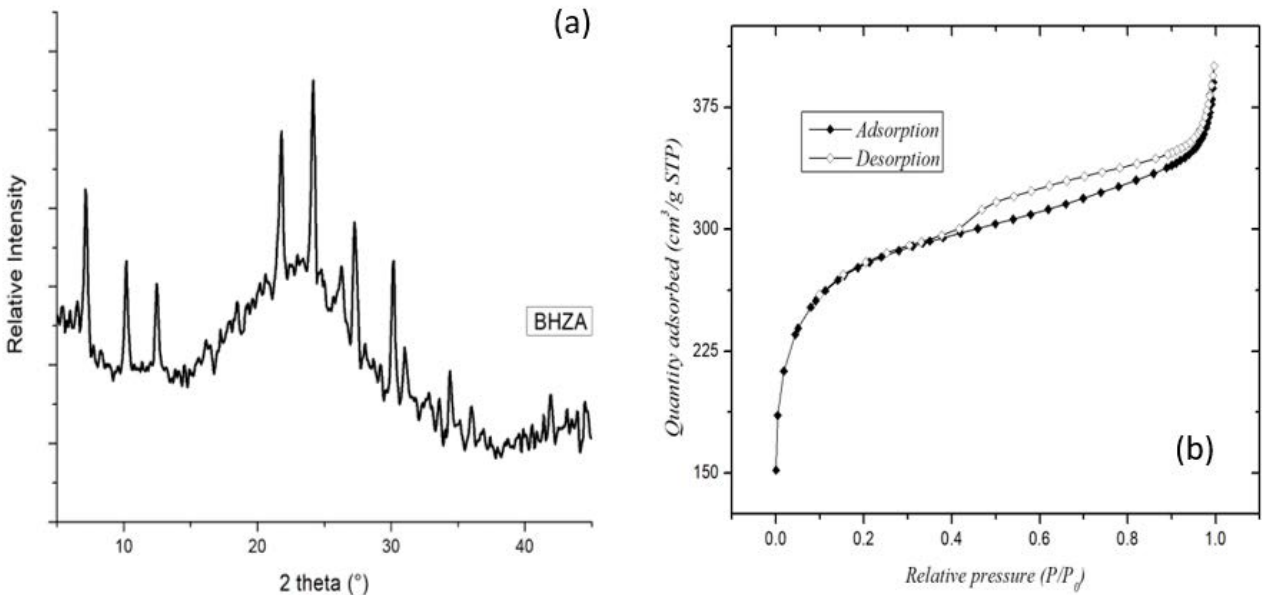

Fig. 6. (a) XRD pattern of produced zeolite/carbon composite BHZA and (b) N_2 physisorption of BHZA.

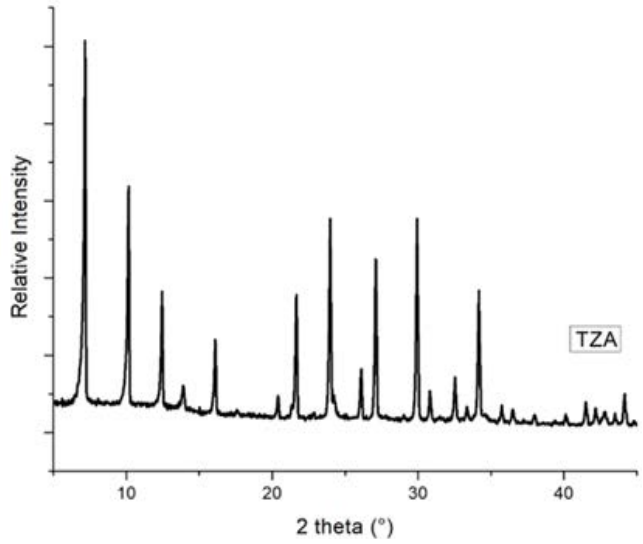

Fig. 7. XRD pattern of zeolite A traditionally produced TZA.

could be very low because they did not clearly appear in the XRD pattern. Other authors have found similar results [38]; Cardoso and co-workers [39] found that the presence of iron oxide as an impurity in the raw material for the synthesis of a zeolite type Na-P affects the *zeolitization* processes, which lead to the formation or undesirable crystalline phases. On the other hand, Fig. 8(c) shows the N_2 adsorption/desorption isotherm of ZA. The surface area suffered an important decrease from 28.6 to 7.88 m^2 g^{-1} as summarized in Table 1. This effect can be associated with the removal of carbon responsible for larger surface area after the calcination process. Also, the pore volume decreased from 0.27 to 0.05 cm^3 g^{-1}, which can be explained by the presence of different elements such as minerals other than zeolitic porous materials, as previous EDX analysis revealed.

3.2. Adsorption tests – kinetics

Fig. 9 shows the experimental results of the adsorption kinetics of Cu ions (400 mg L^{-1}, pH 4) at 25°C onto BHC, BHZA, ZA, and TZA. The results indicate that copper removal increased with time and equilibrium stage at approximately 20 min was achieved for all compared materials. Poor copper adsorption was observed using BHC, up to 4.7 mg L^{-1}; meanwhile, BHZA and ZA present 22.1 and 31.8 mg L^{-1}, respectively. Although ZA adsorption capacity is greater than BHZA, up to 30.5%, it is considered that this zeolite possesses a hierarchical structure, which has the ability to prevent agglomeration of powders in suspension that can block active surface area [39]. TZA showed to have a superior capacity than all prepared materials under the described conditions, 72 mg L^{-1}.

In order to study the adsorption kinetics of copper ions using BHC, BHZA, ZA, and TZA, PFO and PSO models were used. The corresponding predicted values are presented in Fig. 10. According to Miyake et al. [39], the kinetic constant k_1 is dependent only on the relationship between the sorption rate and the ion concentration in solution. On the other hand, PSO model suggests that the rate-limiting steps are the chemical interactions and the sorptive process depends on the available active sites on the solid surface [40,41]. The estimated kinetic parameters are shown in Table 2.

A comparison between the PFO and PSO kinetic models suggests that Cu^{2+} adsorption by BHC, BHZA, and TZA closely follows the PFO model (R^2 > 0.979). This result suggests that removal of copper ions depends more on copper ion concentration than on active sites on surface such as the case of ZA (R^2 > 0.989). These results are in agreement with previous results using zeolites and carbonized supports where pure zeolite fits better with the PSO than PFO model [37]. A summary of kinetic results is shown in Table 3.

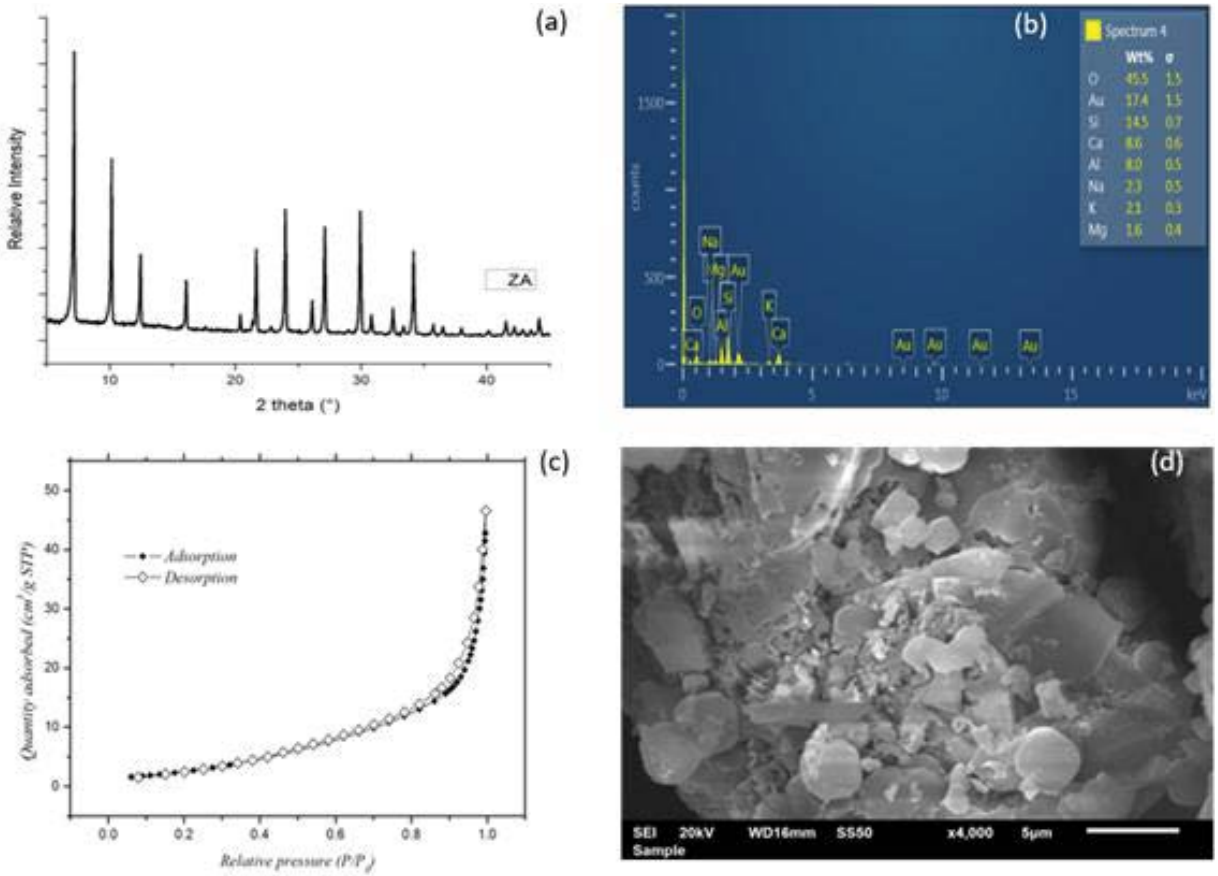

Fig. 8. (a) XRD pattern of ZA, (b) EDX spectrum of ZA, (c) N_2 physisorption of ZA, and (d) SEM image of ZA.

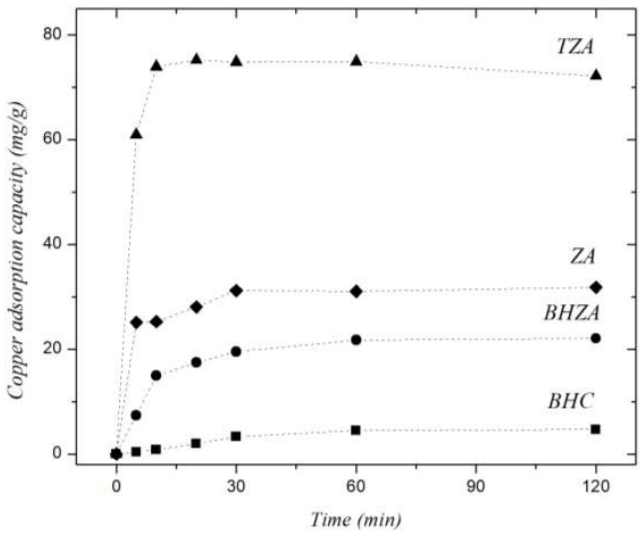

Fig. 9. Kinetic behavior of BHC, BHZA, ZA, and TZA.

3.3. Adsorption tests – equilibrium

In order to compare directly the zeolite prepared using agro-industrial wastes in this work (ZA) with the traditionally prepared ZA (TZA), the copper adsorption isotherms (at 25°C and pH 4) are presented in Fig. 11. The results show that the quantity of copper adsorbed onto TZA is greater (145.07 mg L^{-1}) than that by ZA (85.71 mg L^{-1}) for the given conditions and initial concentration range. The differences between the adsorption capacities of TZA and ZA could be explained on the basis of the different synthesis methodology and a different material composition. As in kinetic studies, the TZA achieved superior adsorption capacity.

The maximum experimental adsorption capacity of copper onto zeolitic materials synthetized in this research is similar to or higher than those reported for other zeolites, both natural and synthetic, such as NaA [42], NaX [43], Na-Clinoptilolite [44], and Fe-Clinoptilolite [45], in which the reported adsorptive capacities ranged from 13.4 to 124.3 mg L^{-1}. According to the Langmuir model, the q_{max} values, i.e., maximum theoretical adsorption capacity at equilibrium for pure ZA, were 121.07 and 187 mg g^{-1} for

Table 2
Textural properties of BHC, BHZA, and ZA

Material	S_{BET} (m^2 g^{-1})	Single point surface area (m^2 g^{-1})	Pore diameter (nm)	Pore volume (cm^3 g^{-1})
BHC	40.7	1,362.8	2.63	0.21
BHZA	28.6	868.5	3.18	0.27
ZA	7.88	174.6	5.94	0.05

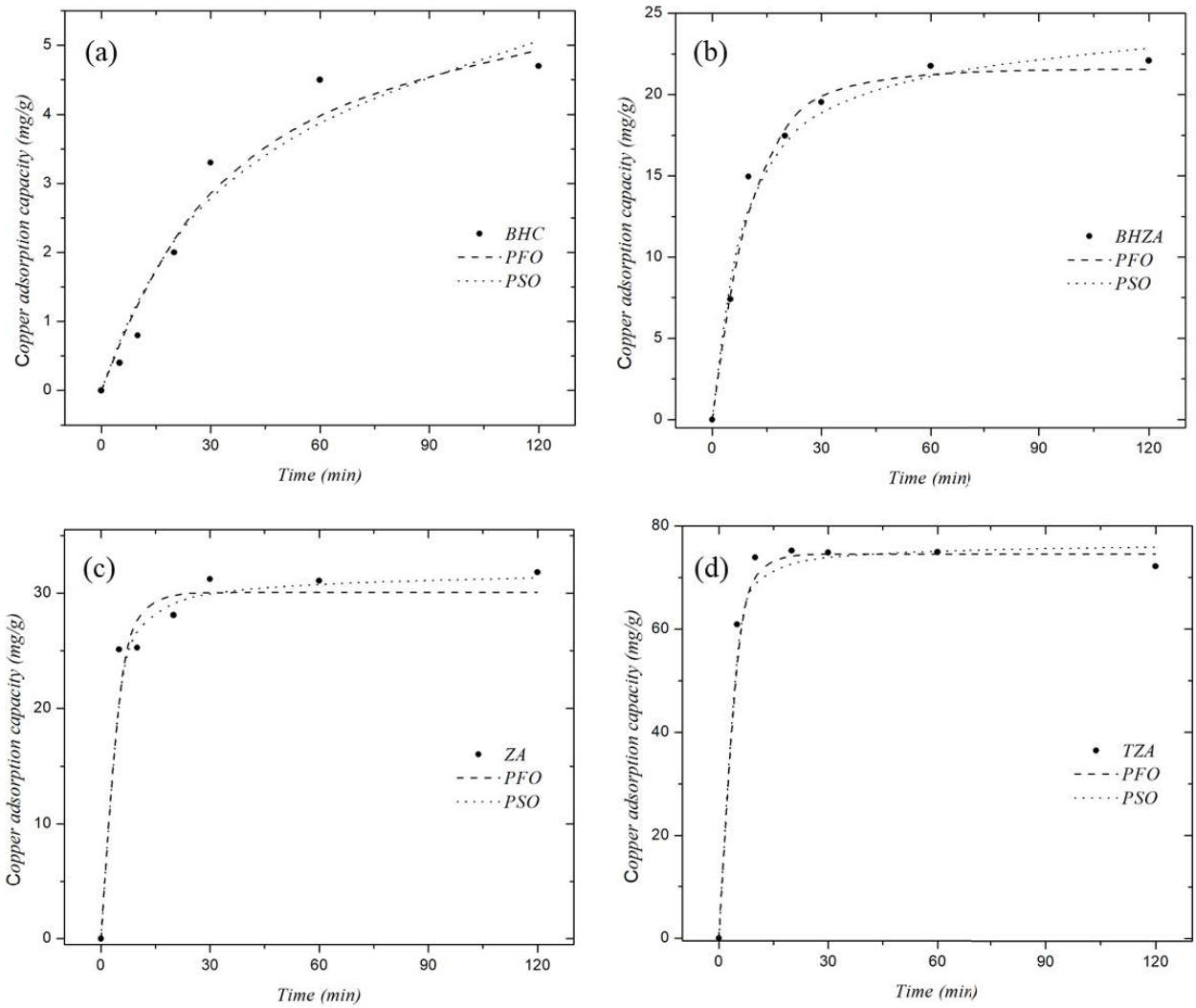

Fig. 10. Pseudo-first-order vs pseudo-second-order models for (a) BHC, (b) BHZA, (c) ZA, and (d) TZA. Dotted lines represent the correspondent model.

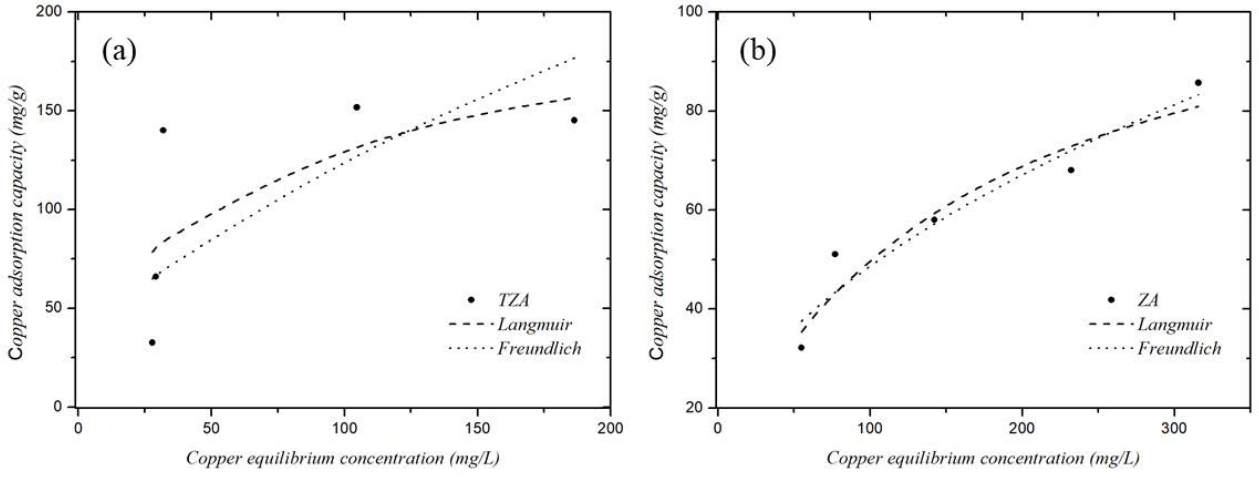

Fig. 11. Copper adsorption isotherms using TZA and ZA. Dotted lines represent the corresponding theoretical model.

Table 3
Kinetic parameters of BHC, BHZA, TZA, and ZA

Material	Pseudo-first order			Pseudo-second order		
	q_{PFO}, mg g^{-1}	k_1, min^{-1}	R^2	q_{PSO}, mg g^{-1}	k_2, g mg^{-1} min^{-1}	R^2
BHC	5.0961	0.0286	0.977	6.838	0.0035	0.961
BHZA	21.558	0.0957	0.987	24.409	0.0050	0.984
TZA	74.593	0.3479	0.998	76.536	0.0134	0.990
ZA	30.066	0.3072	0.970	31.763	0.0188	0.989

Table 4
Langmuir and Freundlich adsorption isotherm parameters for copper adsorption

Material	Langmuir			Freundlich		
	$q_{m,L}$, mg g^{-1}	K_L, L mg^{-1}	R^2	k_n, mg$^{1-1/n}$ L$^{1/n}$g^{-1}	n_F	R^2
TZA	187.11	0.018	0.5068	41.78	4.199	0.4753
ZA	121.07	0.006	0.9237	8.49	2.49	0.9330

TZA. The obtained parameters for Langmuir and Freundlich models after the experimental adsorption data fittings are summarized in Table 4. For TZA, the approximation of Langmuir model to experimental data is better than that for the Freundlich model according to its corresponding correlation coefficient (Table 4). In the case of ZA, both models have similar correlation coefficients. Langmuir's model assumes that the solid adsorbent has a distribution of number of sites energetically equivalent, and when a layer of one molecule thick (monolayer) is covering the surface, no more accumulation can be done [34]. Otherwise, the Freundlich model considers the formation of multilayers, i.e., sorbate molecules can pileup once monolayer has been formed. Also, Freundlich assumes an energetically heterogenous surface [9]. Thus, this could suggest that during the copper ion adsorption onto TZA and ZA, a combination of both phenomena, mono- and multilayers that can be attributed to a heterogeneity of sites in both materials, occurs.

4. Conclusions

In this work, an agro-industrial residue such as barley husk was revalorized to produce ZA crystals. The content of available silicon in barley husk makes it a viable alternative to be applied in hydrothermal routes in the form of SiO_2 precursors.

The characterization techniques confirmed the successful preparation of ZA following a two-step route: (1) the removal of volatile compounds following a thermal treatment letting silicon available to react with aluminum oxide precursors and (2) the LTA crystal formation by the hydrothermal method.

The prepared material can be used as an environmental technology agent in the adsorption of heavy metals such as copper. Kinetic studies revealed a fast adsorption process (~20 min) for all materials. Also, PSO better described the process for pure zeolite and PFO for the rest of materials evaluated in this study. The high amount of copper (121.07 mg L^{-1}) that can be adsorbed by the prepared material makes it a low cost and straightforward alternative to immobilize copper from aqueous media. It is noticeable that ZA presents a reduction up to 35% in its adsorption capacity if compared with typical ZA, explained in part by the presence of additional matter that does not form part of the hydrothermal process. However, ZA produced from a costless agro-industrial residue can be directly compared with other adsorbents where chemical precursors are used.

Acknowledgments

Authors wish to thank the School of Chemistry (FCQ) at Universidad Autónoma de Nuevo León (UANL), the Zacatecas Council for Science and Technology (COZCyT), and Dr. Geraint Minton for all the support.

References

[1] N.K. Srivastava, C.B. Majumder, Novel biofiltration methods for the treatment of heavy metals from industrial wastewater, J. Hazard. Mater., 151 (2008) 1–8.
[2] A. Fairbrother, R. Wenstel, K. Sappington, W. Wood, Framework for metals risk assessment, Ecotoxicol. Environ. Saf., 68 (2007) 145–227.
[3] P.B. Tchounwou, C.G. Yedjou, A.K. Patlolla, D.J. Sutton, Heavy metal toxicity and the environment, EXS, 101 (2012) 133–164.
[4] M.A.A. Wijayawardena, M. Megharaj, R. Naidu, Exposure, toxicity, health impacts, and bioavailability of heavy metal mixtures, Adv. Agron., 138 (2016) 175–234.
[5] T.A. Kurniawan, G.Y.S. Chan, W.-H. Lo, S. Babel, Physico–chemical treatment techniques for wastewater laden with heavy metals, Chem. Eng. J., 118 (2006) 83–98.
[6] A. Pal, Copper toxicity induced hepatocerebral and neurodegenerative diseases: an urgent need for prognostic biomarkers, Neurotoxicology, 40 (2014) 97–101.
[7] D.G. Barceloux, D. Barceloux, Copper, J. Toxicol. Clin. Toxicol., 37 (1999) 217–230.
[8] S. Dudka, D.C. Adriano, Environmental impacts of metal ore mining and processing: a review, J. Environ. Qual., 26 (1997) 590–596.

[9] V.J. Inglezakis, S.G. Poulopoulos, Adsorption, Ion exchange and Catalysis: Design of Operations and Environmental Applications, Elsevier, 2006.
[10] R. Xu, W. Pang, J. Yu, Q. Huo, J. Chen, Chemistry of Zeolites and Related Porous Materials: Synthesis and Structure, John Wiley & Sons, 2009.
[11] C. Baerlocher, L. McCusker, D. Olson, Atlas of Zeolite Framework Types, Elsevier Science, Amsterdam, 2007.
[12] O.H. Elsayed-Ali, T. Abdel-Fattah, H.E. Elsayed-Ali, Copper cation removal in an electrokinetic cell containing zeolite, J. Hazard. Mater., 185 (2011) 1550–1557.
[13] C.S. Cundy, P.A. Cox, The hydrothermal synthesis of zeolites: precursors, intermediates and reaction mechanism, Microporous Mesoporous Mater., 82 (2005) 1–78.
[14] E.P. Ng, H. Awala, K.H. Tan, F. Adam, R. Retoux, S. Mintova, EMT-type zeolite nanocrystals synthesized from rice husk, Microporous Mesoporous Mater., 204 (2015) 204–209.
[15] J. Parfitt, M. Barthel, S. Macnaughton, Food waste within food supply chains: quantification and potential for change to 2050, Philos. Trans. R. Soc. Lond. B. Biol. Sci., 365 (2010) 3065–3081.
[16] R.M. Mohamed, I.A. Mkhalid, M.A. Barakat, Rice husk ash as a renewable source for the production of zeolite NaY and its characterization, Arabian J. Chem., 8 (2015) 48–53.
[17] C.Y.M. dos Santos, D. de A. Azevedo, F.R. de Aquino Neto, Selected organic compounds from biomass burning found in the atmospheric particulate matter over sugarcane plantation areas, Atmos. Environ., 36 (2002) 3009–3019.
[18] D.I. Petkowicz, R.T. Rigo, C. Radtke, S.B. Pergher, J.H.Z. dos Santos, Zeolite NaA from Brazilian chrysotile and rice husk, Microporous Mesoporous Mater., 116 (2008) 548–554.
[19] P.K. Bajpai, M.S. Rao, K.V.G.K. Gokhale, Synthesis of mordenite type zeolite using silica from rice husk ash, Ind. Eng. Chem. Prod. Res. Dev., 20 (1981) 721–726.
[20] D. Prasetyoko, Z. Ramli, S. Endud, H. Hamdan, B. Sulikowski, Conversion of rice husk ash to zeolite beta, Waste Manage., 26 (2006) 1173–1179.
[21] S.-F. Wong, H. Awala, A. Vincente, R. Retoux, T.C. Ling, S. Mintova, R.R. Mukti, E.-P. Ng, K-F zeolite nanocrystals synthesized from organic-template-free precursor mixture, Microporous Mesoporous Mater., 249 (2017) 105–110.
[22] K.P. Dey, S. Ghosh, M.K. Naskar, Organic template-free synthesis of ZSM-5 zeolite particles using rice husk ash as silica source, Ceram. Int., 39 (2013) 2153–2157.
[23] B.S. Liu, D.C. Tang, C.T. Au, Fabrication of analcime zeolite fibers by hydrothermal synthesis, Microporous Mesoporous Mater., 86 (2005) 106–111.
[24] D.A. Fungaro, T.V.S. Reis, M. Antonio Logli, N.A. Oliveira, Synthesis and characterization of zeolitic material derived from sugarcane straw ash, Am. J. Environ. Prot., 2 (2014) 16–21.
[25] S. Salakhum, T. Yutthalekha, M. Chareonpanich, J. Limtrakul, C. Wattanakit, Synthesis of hierarchical faujasite nanosheets from corn cob ash-derived nanosilica as efficient catalysts for hydrogenation of lignin-derived alkylphenols, Microporous Mesoporous Mater., 258 (2018) 141–150.
[26] M.M.M. Ali, M.J. Ahmed, Adsorption behavior of doxycycline antibiotic on NaY zeolite from wheat (Triticum aestivum) straws ash, J. Taiwan Inst. Chem. Eng., 81 (2017) 218–224.
[27] E.-P. Ng, J.-H. Chow, R.R. Mukti, O. Muraza, T.C. Ling, K.-L. Wong, Hydrothermal synthesis of zeolite a from bamboo leaf biomass and its catalytic activity in cyanoethylation of methanol under autogenic pressure and air conditions, Mater. Chem. Phys., 201 (2017) 78–85.
[28] E. Fortunati, P. Benincasa, G.M. Balestra, F. Luzi, A. Mazzaglia, D. Del Buono, D. Puglia, L. Torre, Revalorization of barley straw and husk as precursors for cellulose nanocrystals extraction and their effect on PVA_CH nanocomposites, Ind. Crops Prod., 92 (2016) 201–217.
[29] S.N. Azizi, A.R. Dehnavi, A. Joorabdoozha, Synthesis and characterization of LTA nanozeolite using barley husk silica: mercury removal from standard and real solutions, Mater. Res. Bull., 48 (2013) 1753–1759.
[30] D.A. De Haro-Del Rio, S.M. Al-Jubouri, S.M. Holmes, Hierarchical porous structured zeolite composite for removal of ionic contaminants from waste streams, Chim. Oggi-Chem. Today, 35 (2017) 56–58.
[31] Y.S. Ho, Citation review of Lagergren kinetic rate equation on adsorption reactions, Scientometrics, 59 (2004) 171–177.
[32] Y.S. Ho, G. McKay, The kinetics of sorption of divalent metal ions onto sphagnum moss peat, Water Res., 34 (2000) 735–742.
[33] N.Z. Misak, Langmuir isotherm and its application in ion-exchange reactions, React. Polym., 21 (1993) 53–64.
[34] J. Febrianto, A.N. Kosasih, J. Sunarso, Y.H. Ju, N. Indraswati, S. Ismadji, Equilibrium and kinetic studies in adsorption of heavy metals using biosorbent: a summary of recent studies, J. Hazard. Mater., 162 (2009) 616–645.
[35] S.V. Vassilev, C.G. Vassileva, Y.C. Song, W.Y. Li, J. Feng, Ash contents and ash-forming elements of biomass and their significance for solid biofuel combustion, Fuel, 208 (2017) 377–409.
[36] O. Hernandez-Ramirez, S.K. Al-Nasri, S.M. Holmes, Hierarchical structures based on natural carbons and zeolites, J. Mater. Chem., 21 (2011) 16529–16534.
[37] D.A. De Haro-Del Rio, S. Al-Joubori, O. Kontogiannis, D. Papadatos-Gigantes, O. Ajayi, C. Li, S.M. Holmes, The removal of caesium ions using supported clinoptilolite, J. Hazard. Mater., 289 (2015) 1–8.
[38] C. Belviso, F. Cavalcante, A. Lettino, S. Fiore, A and X-type zeolites synthesised from kaolinite at low temperature, Appl. Clay Sci., 80 (2013) 162–168.
[39] A.M. Cardoso, A. Paprocki, L.S. Ferret, C.M. Azevedo, M. Pires, Synthesis of zeolite Na-P1 under mild conditions using Brazilian coal fly ash and its application in wastewater treatment, Fuel, 139 (2015) 59–67.
[40] Y. Miyake, H. Ishida, S. Tanaka, S.D. Kolev, Theoretical analysis of the pseudo-second order kinetic model of adsorption. Application to the adsorption of Ag(I) to mesoporous silica microspheres functionalized with thiol groups, Chem. Eng. J., 218 (2013) 350–357.
[41] Y.S. Ho, G. McKay, Pseudo-second order model for sorption processes, Process Biochem., 34 (1999) 451–465.
[42] X. Lu, F. Wang, X. Li, K. Shi, E.Y. Zheng, Adsorption and Thermal Stabilization of Pb^{2+} and Cu^{2+} by Zeolite, Ind. Eng. Chem. Res., 55 (2016) 8767–8773.
[43] X. Lu, D. Shi, J. Chen, Sorption of Cu^{2+} and Co^{2+} using zeolite synthesized from coal gangue: isotherm and kinetic studies, Environ. Earth Sci., 76 (2017) 1–10.
[44] Y. Taamneh, S. Sharadqah, The removal of heavy metals from aqueous solution using natural Jordanian zeolite, Appl. Water Sci., 7 (2017) 2021–2028.
[45] M. Irannajad, H.K. Haghighi, E. Safarzadeh, Kinetic, thermodynamic and equilibrium studies on removal of copper ions from aqueous solutions by natural and modified clinoptilolites, Korean J. Chem. Eng., 55 (2016) 1629–1639.